Sea Ice Change Detection from SAR Images Based on Canonical Correlation Analysis and Contractive Autoencoders

Xiao Wang[1,2], Feng Gao[1,2(✉)], Junyu Dong[1,2], and Shengke Wang[1,2]

[1] College of Information Science and Engineering, Ocean University of China, Qingdao, China
{gaofeng,dongjunyu,neverme}@ouc.edu.cn
[2] Qingdao Key Laboratory of Mixed Reality and Virtual Ocean, Qingdao, China
1195747610@qq.com

Abstract. In this paper, we proposed a novel sea ice change detection method for Synthetic Aperture Radar (SAR) images based on Canonical Correlation Analysis (CCA) and Contractive Autoencoders (SCAEs). To alleviate the effect of multiplicative speckle noise, structured matrix decomposition is utilized for difference image enhancement, and therefore, better difference image with less noisy spots can be obtained. In order to get good data representations in changed and unchanged pixels classification, CCA and SCAEs are combined to exploit more effective changed features. Experiments on two real sea ice datasets demonstrate the robustness and efficiency of the proposed method in comparison with three other state-of-the-art methods.

Keywords: Change detection · Synthetic aperture radar
Canonical correlation analysis · Contractive autoencoders
Remote sensing image

1 Introduction

Sea ice is an important part of the cryosphere that interacts continuously with the underlying oceans and the overlaying atmosphere. Global warming accelerates the loss of sea ice, which threatens animals living in the Polar Regions [1]. In addition, polar sea ice information is very important for safe navigation, since the amount of ice adversely impacts the friction against the hull of a vessel. Therefore, polar sea ice research has attracting increasing attentions and raised global security concerns these years.

More and more Synthetic Aperture Radar (SAR) sensors have been developed, and a large number of multitemporal image pairs have been acquired in

This work was supported by the National Natural Science Foundation of China (Grant Nos. 41606198 and 41576011) and in part by the Shandong Province Natural Science Foundation of China under Grant No. ZR2016FB02.

R. Hong et al. (Eds.): PCM 2018, LNCS 11165, pp. 748–757, 2018.
https://doi.org/10.1007/978-3-030-00767-6_69

the past decades. SAR images provides the capabilities for all-weather, day-and-night surveillance. The applications of SAR images has become a hot research topic in remote sensing communities. Among these applications, sea ice monitoring is an essential issue. However, sea ice change detection from SAR images exhibits difficulties due to the presence of multiplicative speckle noise [8]. How to alleviate the interference of speckle noise has become a critical issue in sea ice change detection from SAR images.

In general, change detection [2] consists of three main steps: (1) image preprocessing; (2) difference image (DI) generation from a pair of multitemporal images; (3) DI analysis to achieve the segmentation of the changed regions. The first step mainly includes geometric correction and denoising. Some methods have been employed to alleviate the effect to speckle noise, e.g., Gamma-MAP [3] and SRAD [4]. In the second step, the log-ratio operator is usually employed since it is considered to be robust to the speckle noise [5]. In this paper, the log-ratio operator is employed for DI generation. In the final step, clustering methods are very popular, since they do not require DI image distribution. Celik [6] used the principal component analysis (PCA) and k-means clustering for classification. Gao et al. [7] use Gabor wavelets and fuzzy c-means (FCM) algorithm to select samples for classification. Gong et al. [8] proposed a reformulated fuzzy local-information c-means clustering algorithm for classifying changed and unchanged regions in the generated DI. These clustering methods gain satisfying performance and are popular in the past decades. However, clustering methods are sensitive to initial values, and improper initial values may result in premature convergence on local optima.

In recent years, deep learning shows its dominant performance in many fields, such as image classification [9], voice recognition [10] and nature language processing, etc. In [11], Wang et al. demonstrated that convolution neural network (CNN) has been used to estimate ice concentration using SAR scenes captured during the melt season. In [12], a deep neural network is established for SAR image change detection. It is empirically verified that deep learning can further improve the change detection performance.

The above mentioned methods have gain good performance in SAR image change detection. However, there are still two problems to be considered: (1) The speckle noise should be suppressed in the process of DI generation; (2) Good data representations should be achieved from multitemporal images to identify changed regions. With respect to the first problem, in this paper, Structured Matrix Decomposition (SMD) is utilized for DI enhancement, and therefore better DI with less noisy spots can be obtained. To solve the second problem, we develop a classification model based on Canonical Correlation Analysis and Contractive Autoencoders (CCA-SCAEs) to exploit good representations from multitemporal SAR images.

The main contributions of the proposed method are listed as follows: First, SMD is introduced to suppress the speckle noise to obtain DI with less noisy spots. Saliency detection method can capture the distinctive patterns and suppress the background noise, but it is rarely considered in change detection.

Second, a novel classification model based on CCA and SCAEs is established to exploit change information from multitemporal SAR images. Experimental results on two real SAR datasets demonstrate the effectiveness of the proposed method.

The remainder of this paper is organized as follows: Sect. 2 presents the change detection problem statements and describes the proposed method in details. Section 3 shows the experimental results and the paper closes with a conclusion in Sect. 4.

2 Proposed Method

Given two multitemporal sea ice images I_1 and I_2, which are acquired at the same location but at different times t_1 and t_2. The aim of sea ice change detection is to generate a change map, which gives the interpretations about the changes occurred. The framework of the proposed method is illustrated in Fig. 1.

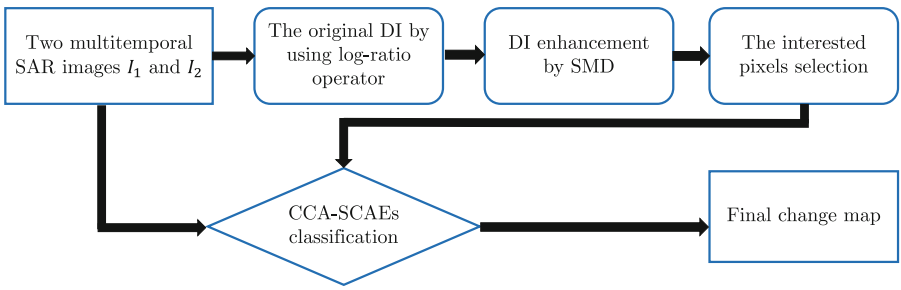

Fig. 1. Framework of the proposed change detection method

Our proposed method is illustrated in Fig. 1, which is mainly comprised of two steps:

Step 1 – DI generation and enhancement. Given two multitemporal images I_1 and I_2, the log-ratio operator is employed to obtain an initial DI. In order to remove speckle noise spots, we use the SMD method to enhanced the DI and suppress the speckle noise.

Step 2 – Training samples generation and classification. We need reliable samples for the classification model. Hierarchical FCM clustering algorithm [7] is used for reliable samples generation. Then, a classifier based on CCA and SCAEs will be built. The changed regions can be identified by feeding pixels from multitemporal images into the classifier. Then, the final change map can be obtained.

2.1 DI Generation and Enhancement

The log-ratio operator is chosen to obtain an initial DI. We choose log-ratio operator since it is empirically verified to be capable to reduce the speckle noise

to some extent. The log-ratio operator is defined as DI $= \log(I_1/I_2)$. However, it is a challenging task to find the interested and distinctive areas from SAR images, which includes many speckle noise spots. Based on this, we should find a better way to improve DI robustness. Saliency map shows interested areas which has a strong contrast with the entire image. Inspired by this, we use saliency detection methods to enhance the DI. Figure 2 shows the similarity between the DI and the saliency map. Figure 2(a) and (b) are the original multitemporal images. Figure 2(c) is the original DI obtained by using the log-ratio operator, which contains many noisy spots. Figure 2(d) is the saliency map, which has less speckle noise spots compared with the original DI.

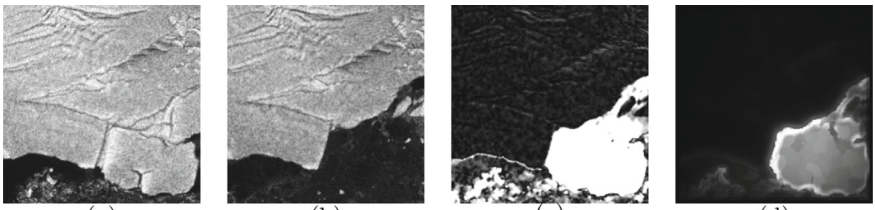

Fig. 2. The similarity between the original DI and the saliency map. (a) and (b) are two original multitemporal images. (c) The original DI obtained by using log-ratio operator. (d) The saliency map acquired by SMD.

In this paper, saliency detection methods based on Structured Matrix Decomposition [13] is utilized. The SMD is defined as follows:

$$\min_{L,S} \varphi(L) + \alpha\Omega(S) + \beta\theta(L,S) \quad s.t. \quad F = L + S, \tag{1}$$

where $\varphi(\cdot)$ is a low-rank constraint to allow identification of the intrinsic feature subspace of the redundant background patches, $\Omega(\cdot)$ is a structured sparsity regularization to capture the spatial and feature relations of patches in S, $\theta(\cdot)$ is an interactive regularization term to enlarge the distance between the subspaces drawn from L and S, and α, β are positive tradeoff parameters. Detailed information about SMD can be found in Peng's work [13].

Let I_D represents the initial DI, and I_{SMD} represent the saliency map obtained by the SMD method, the enhanced difference image I_E is computed by:

$$I_E = \exp(k \cdot I_{SMD}) \cdot I_D, \tag{2}$$

In our implementations, we found that the I_{SMD} is of great significance. Therefore, we use an exponential function to emphasize I_{SMD}. In our implementations, we use $k = 0.2$ as the scaling factor.

After obtaining I_E, we partition the pixels in DI into three groups by using the hierarchical FCM algorihtm [7]: changed class Ω_c, unchanged class Ω_u, and intermediate class Ω_i. Pixels belonging to Ω_c and Ω_u have high probabilities

to be changed or unchanged. These pixels are selected as reliable samples for CCA-SCAEs. The classification model will be introduced in the next subsection in detail.

2.2 Classification via CCA-SCAEs Classifier

Deep learning is a hot topic in recent years and achieves extraordinary results in many fields. The motivation of deep learning is to establish and simulate the neural network of human brain for analysis and learning. It imitates the mechanism of the human brain to explain the data. In this paper, in order to acquire discriminative representation of changed features, neighborhood pixels features of multitemporal SAR images are fed into CCA-SCAEs to learn more effective changed features.

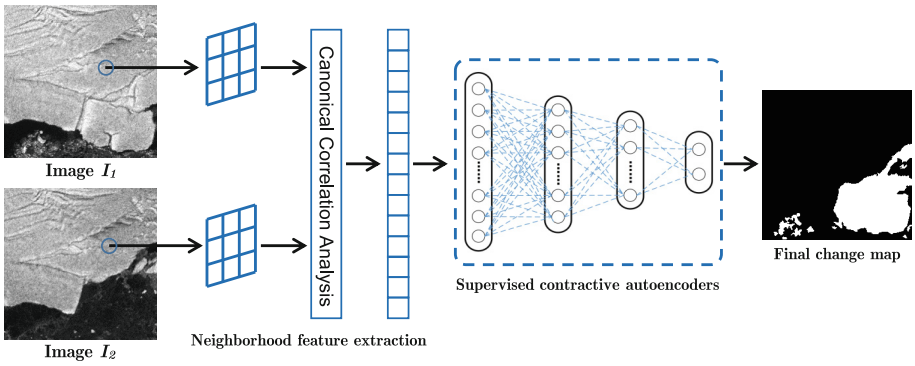

Fig. 3. The proposed classification framework based on Canonical Correlation Analysis and Contractive Autoencoders (CCA-SCAEs).

The framework of CCA-SCAEs is illustrated in Fig. 3. Neighborhood pixel features of multi-temporal SAR images are first processed by canonical correlation analysis (CCA). Then, the obtained features are fed into supervised contractive autoencoders (SCAEs) to learn more effective changed features. Suppose an L layer network, the front $L-1$ layers consist of SCAEs and the top layer is sigmoid function. As for the lth layer with the parameters $\theta^l = \{W_1^l, W_2^l, b_1^l, b_2^l\}$, the training process can be divided into two stages: pretraining and updating [14]. The pretraining objective function is formulated as:

$$J_{\text{pre}}^l(\theta^l) = \frac{1}{2N}\sum_{i=1}^{N}\left\{\|\hat{x}_i^l - h_i^{l-1}\|_2^2 + \lambda\sum_{j=1}^{n_l}(h_{ij}^l(1-h_{ij}^l))^2\|W_{1j}^l\|_2^2\right\} + \frac{\delta}{2}\|W_1^l\|_F^2, \tag{3}$$

where the first term represent the reconstruction error, the second term denotes the contractive penalty to optimize the encoding function, and the third term stands for the weight decay of the parameters. After pretraining, multinomial logistic regression module is connected with the encoder to update the parameters of SCAE. The updating function is written as:

$$J^l_{\text{update}}(\theta^l) = -\frac{1}{N}\sum_{i=1}^{N} y_i \log p_i^l + \frac{\tau}{2}\|W_2^l\|_F^2 \tag{4}$$

where the first term is used to capture the relevant information between features and labels, and the second term denotes the weight decay. After training of each SCAE, the whole network is fine-tuned from the top layer to the final layer. The sigmoid function on the top layer is applied to classify each pixel into changed and unchanged class.

3 Experimental Results and Analysis

3.1 Datasets Description

In this section, we evaluate the performance of the proposed method on two real datasets, which are acquired from two large SAR images of the region of the Sulzberger Ice Shelf. Both of two SAR images, which have the size of 2263 $\times$ 2264 pixels, are provided by the European Space Agency's Envisat satellite on March 11 and 16, 2011. It is huge to us, so we selected a part of these images, which area is 256 $\times$ 256 pixels. Both datasets are shown in Figs. 4 and 5. (a) and (b) are the original images and (c) is the ground truth image, which are obtained by integrating prior information with photo interpretation.

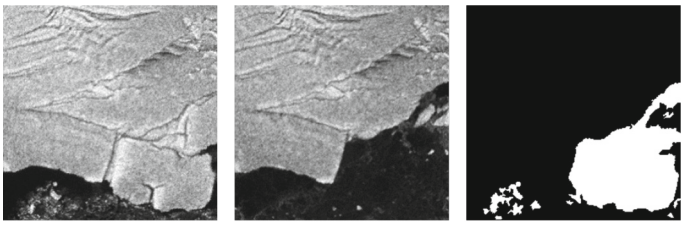

Fig. 4. Dataset I from Sulzerger Ice Shelf. (a) Image acquired in March 11 in 2011. (b) Image acquired in March 16 in 2011. (c) Ground truth image obtained by integrating prior information with photo interpretation.

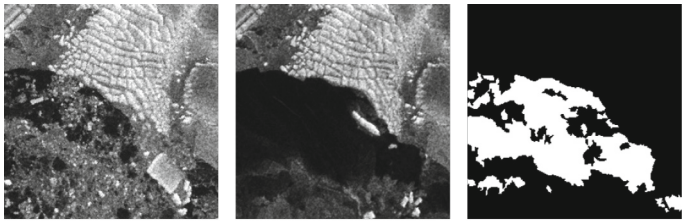

(a) (b) (c)

Fig. 5. Dataset II from Sulzerger Ice Shelf. (a) Image acquired in March 11 in 2011. (b) Image acquired in March 16 in 2011. (c) Ground truth image obtained by integrating prior information with photo interpretation.

3.2 Evaluation Criteria

In order to prove the effectiveness of the proposed method, we introduce five criteria to evaluate the performance of experimental results, such as false positives (FP), false negatives (FN), overall error (OE), percentage correct classification (PCC) and Kappa coefficient (KC). FP is the number of pixels belong to the unchanged class in the ground truth image but wrongly classified as the changed class. On the contrary, FN is the number of pixels belong to the changed class in the ground truth image but wrongly classified as the unchanged class. OE represents the sum of FP and FN. PCC is the percentage correct classification of the algorithm and its representation can be defined as follows:

$$\mathrm{PCC} = \frac{N - \mathrm{FP} - \mathrm{FN}}{N} \times 100\% \tag{5}$$

where N is the total number of pixels in the images. The KC is a critical measurement of change detection accuracy, and it is a more persuasive coefficient because more detailed information is involved.

3.3 Experimental Results on Dataset I

In this paper, we compare our algorithm with other three state-of-the-art methods: PCAKM [6], GaborTLC [15] and GaborPCANet [7]. And the accuracy of the experiment results is showed in two ways: image change map and tabular form. We first evaluate our proposed method on the Dataset I. Figure 6 shows the final experimental results on Dataset I and Table 1 illustrate the evaluate criteria of different methods. From Fig. 6, we can find that the result of GaborTLC is polluted by many white noisy spots. Many unchanged pixels are wrongly classified into the changed class. Similar conditions can be found in the results of PCAKM and GaborPCANet. The PCC value of the proposed method achieves the best performance on this dataset. It can be concluded that the proposed method can efficiently suppress the multiplicative speckle noise by introducing saliency detection.

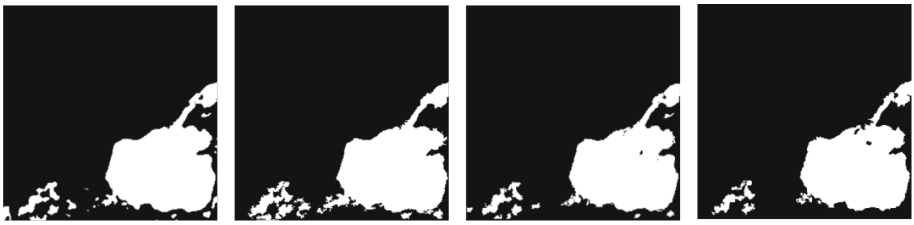

Fig. 6. Experimental results on Dataset I. (a) Result by PCAKM. (b) Result by GaborTLC. (c) Result by GaborPCANet. (d) Result by the proposed method.

Table 1. Change detection results of different methods on Dataset I.

Methods	FP	FN	OE	PCC (%)	KC (%)
PCAKM [6]	711	479	1190	98.18	87.13
GaborTLC [15]	1171	423	1594	97.57	92.39
GaborPCANet [7]	435	833	1268	98.07	93.73
Proposed method	232	930	1162	98.23	94.21

3.4 Experimental Results on Dataset II

We also test the proposed model on the Dataset II. Figure 7 shows the final sea ice change detection results of different methods. It can be observed that the results of PCAKM, GaborTLC and GaborPCANet are relatively inefficient in speckle noise suppression, which lead to the change maps containing many speckle noise spots. Table 2 shows the comparisons of different methods according to the five evaluation criterion. From Table 2, we find that the FP values of different methods are higher than that in the Dataset I. One important reason is that Dataset II contain very complicated background compared with Dataset I, which poses a challenge to change detection and needs the higher robust method

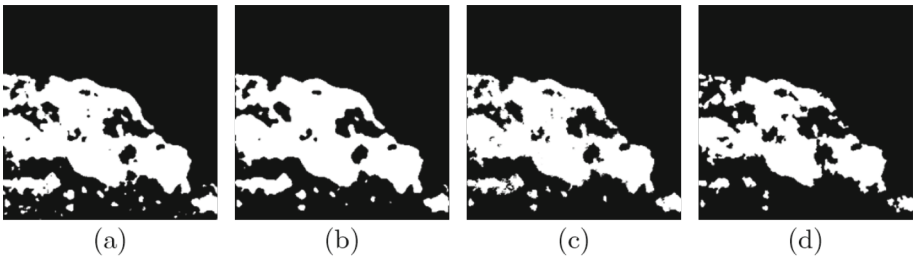

Fig. 7. Experimental results on Dataset I. (a) Result by PCAKM. (b) Result by GaborTLC. (c) Result by GaborPCANet. (d) Result by the proposed method.

Table 2. Change detection results of different methods on Dataset II.

Methods	FP	FN	OE	PCC (%)	KC (%)
PCAKM [6]	3215	141	3356	94.88	87.13
GaborTLC [15]	2805	174	2979	95.44	88.48
GaborPCANet [7]	2237	599	2836	95.67	88.82
Proposed method	889	863	1861	97.16	92.44

to improve the accuracy. The proposed methods produces fewer false alarms and it suppresses the bad effects of multiplicative speckle noise. Both visual and data quantitative comparison on this dataset has demonstrated the effectiveness of the proposed method.

4 Conclusion

In this paper, we proposed a sea ice change detection method from SAR images based on Canonical Correlation Analysis and Contractive Autoencoders (CCA-SCAEs). On the one hand, the structured matrix decomposition can improve the difference image, which has less speckle noise spots for the classification. On the other hand, by using the hierarchical FCM algorithm, some reliable samples can be acquired to train the CCA-SCAEs classifier. Finally, we use the CCA-SCAEs classifier to classify pixels from the original SAR images into changed and unchanged class, and the final change map can be obtained. The proposed method is implemented on two real sea ice datasets. The experimental results have demonstrated the proposed method can efficiently reduce the speckle noise, while also preserving the fine details of change features.

References

1. Wang, L., Scott, K.A., Clausi, D.A.: Sea ice concentration estimation during freeze-up from SAR imagery using a convolutional neural network. Remote Sens. **9**, 409 (2017)
2. Zhang, H., Gong, M., Zhang, P., Su, L., Shi, J.: Feature-level change detection using deep representation and feature change analysis for multispectral imagery. IEEE Geosci. Remote Sens. Lett. **13**, 1666–1670 (2016)
3. Lopes, A., Nezry, E., Touzi, R., Laur, H.: Structure detection and statistical adaptive speckle filtering in SAR images. Int. J. Remote Sens. **14**, 1735–1758 (1993)
4. Gomez, L., Munteanu, C., Berlles, J., Mejail, M.: Evolutionary expert-supervised despeckled SRAD filter design for enhancing SAR images. IEEE Geosci. Remote Sens. Lett. **8**, 814–818 (2011)
5. Bazi, Y., Bruzzone, L., Melgani, F.: An unsupervised approach based on the generalized Gaussian model to automatic change detection in multitemporal SAR images. IEEE Trans. Geosci. Remote Sens. **43**, 874–887 (2005)

6. Celik, T.: Unsupervised change detection in satellite images using principal component analysis and k-means clustering. IEEE Geosci. Remote Sens. Lett. **6**, 772–776 (2009)
7. Gao, F., Dong, J., Li, B., Xu, Q.: Automatic change detection in synthetic aperture radar images based on PCANet. IEEE Geosci. Remote Sens. Lett. **13**, 1792–1796 (2016)
8. Gong, M., Zhou, Z., Ma, J.: Change detection in synthetic aperture radar images based on image fusion and fuzzy clustering. IEEE Trans. Image Process. **21**, 2141–2151 (2012)
9. Lin, K., Lu, J., Chen, C.-S., Zhou, J.: Learning compact binary descriptors with unsupervised deep neural networks. In: IEEE Conference on Computer Vision and Pattern Recognition (CVPR), pp. 1183–1192 (2016)
10. Sell, G., Garcia-Romero, D., McCree, A.: Speaker diarization with I-Vectors from DNN senone posteriors. In: Proceedings of Interspeech, pp. 3096–3099 (2015)
11. Wang, L., Scott, K.A., Xu, L., et al.: Sea ice concentration estimation during melt from dual-pol SAR scenes using deep convolutional neural networks: a case study. IEEE Trans. Geosci. Remote Sens. **54**, 4524–4533 (2016)
12. Gong, M., Zhao, J., Liu, J., Miao, Q., Jiao, L.: Change detection in synthetic aperture radar images based on deep neural networks. IEEE Trans. Neural Netw. Lear. Syst. **27**, 125–138 (2016)
13. Peng, H., Li, B., Ling, H., Hu, W., Xiong, W., Maybank, S.: Salient object detection via structured matrix decomposition. IEEE Trans. Patter. Anal. Mach. Intell. **39**, 818–832 (2017)
14. Geng, J., Wang, H., Fan, J., Ma, X.: Deep supervised and contractive neural network for SAR image classificaiton. IEEE Trans. Geosci. Remote Sens. **55**, 2442–2459 (2017)
15. Li, H., Celik, T., Longbotham, N.: Gabor feature based unsupervised change detection of multitemporal SAR images based on two-level clustering. IEEE Geosci. Remote Sens. Lett. **12**, 2458–2462 (2015)